Acta Oto-Laryngologica, 2009; 129: 45–51

informa
healthcare

ORIGINAL ARTICLE

Effects of hypergravity on histamine H1 receptor mRNA expression in hypothalamus and brainstem of rats: implications for development of motion sickness

GO SATO[1], ATSUHIKO UNO[3], ARATA HORII[3], HAYATO UMEHARA[2], YOSHIAKI KITAMURA[1], KAZUNORI SEKINE[1], KOICHI TAMURA[1], HIROYUKI FUKUI[2] & NORIAKI TAKEDA[1]

[1]*Department of Otolaryngology,* [2]*Department of Molecular Pharmacology, Institute of Health Biosciences, University of Tokushima Graduate School, Tokushima and* [3]*Department of Otolaryngology, Osaka University School of Medicine, Osaka, Japan*

Abstract

Conclusion: The study findings suggest that histamine was released from the axon terminals in the hypothalamus and brainstem and the released histamine activated post-synaptic H1 receptors there, resulting in the development of motion sickness. *Objectives:* We first examined which subtype of post-synaptic histaminergic receptor was responsible for the development of motion sickness. We then examined whether H1 receptors were up-regulated in various areas of the rat brain after 2 G hypergravity load, because the stimulation of H1 receptor was reported to up-regulate the level of H1 receptor protein expression through augmentation of H1 receptor mRNA expression. *Materials and methods:* For this purpose, we used an animal model of motion sickness, using pica (eating non-nutritive substances such as kaolin), as a behavioral index in rats. *Results:* After 2 G hypergravity load, rats ate a significant amount of kaolin, indicating that they suffered from motion sickness. The hypergravity-induced kaolin intake was suppressed by mepyramine, but not by terfinadine or zolantizine. This finding indicates that cerebral post-synaptic H1 but not H2 or peripheral H1 receptors play an important role in the development of motion sickness. The expression of H1 receptor mRNA was up-regulated in the hypothalamus and brainstem, but not in the cerebral cortex after 2 G hypergravity load in rats.

Keywords: *Motion sickness, histamine, H1 receptor, kaolin, mepyramine, terfenadine, zolantidine, hypothalamus, brainstem*

Introduction

Humans without vestibular function never suffer from motion sickness, indicating that the vestibular system is essential for the development of motion sickness [1]. H1 blockers are clinically effective in preventing motion sickness [2,3], indicating that the histaminergic neuron system is important in the development of motion sickness. To investigate the vestibulo-histaminergic interaction in the processes of motion sickness, we developed an animal model of motion sickness in rats [4]. Rats cannot vomit, but pica, the intake of non-nutritive substances such as kaolin (hydrated aluminum silicate), is an illness response behavior of rats, which is analogous to vomiting. In the previous study, we showed that motion-induced pica is an index of motion sickness in rats [5].

A 2 G hypergravity load induced kaolin intake in rats, indicating that they suffered from motion sickness [6]. The hypergravity and caloric vestibular stimulation increased the release of histamine from the rat hypothalamus, suggesting that the activation of histaminergic neuron system in the hypothalamus through the vestibulo-histaminergic interaction plays an important role in the development of motion sickness [6,7]. In the present study, to investigate the post-synaptic events after the vestibulo-histaminergic interaction, we first used the animal model and examined which subtype of post-synaptic

Correspondence: Go Sato MD, Department of Otolaryngology, Institute of Health Biosciences, University of Tokushima Graduate School, 3-18-15 Kuramoto, Tokushima 770-8503, Japan. Tel: +81 88 633 7169. Fax: +81 88 633 7170. E-mail: go-sato@clin.med.tokushima-u.ac.jp

(Received 9 January 2008; accepted 24 February 2008)

ISSN 0001-6489 print/ISSN 1651-2251 online
DOI: 10.1080/00016480802008173

histaminergic receptor was responsible for the development of motion sickness. The effects of pretreatment by mepyramine, an H1-blocker, by terfenadine, an H1-blocker that does not cross the blood–brain barrier (BBB) or by zolantidine, a BBB-penetrating H2-blocker, on hypergravity-induced pica were examined in rats.

Recently it was reported that the stimulation of H1 receptor up-regulates the level of H1 receptor protein expression through augmentation of H1 receptor mRNA expression in HeLa cells and rat nasal mucosa [8,9]. These findings led to the idea that the expression of H1 receptor mRNA is increased by 2 G hypergravity load in the brain area to which the histaminergic activation is transmitted in the processes of motion sickness. So, we then examined whether H1 receptors were up-regulated in various areas of the rat brain after 2 G hypergravity load.

Materials and methods

Animals, kaolin preparation, and hypergravity stimulation

All animal experiments were approved by the Animal Care Committee of the University of Tokushima School of Medicine. Male Wistar strain rats weighing 250 g were used. They were kept in individual standard home cages ($35 \times 25 \times 45$ cm) with free access to food, water, and kaolin in a room with a 12 h light/12 h dark cycle (light from 8:30 to 20:30). Their sensitivity to motion sickness was assessed before the experiment and only susceptible animals were used. Accordingly the animals that consumed <1.0 g of kaolin after a 2 h load of hypergravity were excluded from the study, because this experiment was designed to assess the effect of anti-motion sickness drugs.

Pharmaceutical grade kaolin (hydrated aluminum silicate, Ishizu Pharmaceutical Co., Japan) was mixed with 1% arabic gum (Ishizu Pharmaceutical Co.) in distilled water to form a thick paste, which was extruded through a syringe onto wire mesh trays and partially dried at room temperature. This mixture was then introduced into a column of the same shape as that for food, and again dried completely at room temperature. The kaolin, provided in containers, was placed in the cage. The kaolin container was removed, weighed to the nearest 0.1 g, refilled, and replaced at 18:00 each day. Spilt kaolin was collected, dried, and weighed to obtain the correct values for kaolin consumption.

Hypergravity was produced by an animal centrifuge device [6]. The swing arm on which the animal cage was suspended was mounted 50 cm from the axis of a turntable driven by a servo-controlled torque motor. The turntable was rotated at a constant rate, loading the animal in the centrifuge cage with the vector sum of the gravity linear acceleration and a rotation centrifugal linear acceleration vectors. An angular velocity of 336°/s (56 rpm) achieved a resultant linear acceleration of 2 G acting on the animal along its back to abdomen axis.

Effects of histamine receptor blockers on hypergravity-induced kaolin intake

Kaolin was placed in the cage for 3 days before the hypergravity load was applied to allow the animals to become adapted to its presence. Following this adaptation period, animals were exposed to 2 G hypergravity for 2 h on the next day. Seven days after the first hypergravity load, animals were divided into four groups according to the administered drugs: saline group (Sal, $n=6$), mepyramine group (Mep, $n=6$), terfenadine group (Ter, $n=5$), and zolantidine group (Zol, $n=8$). Mepyramine (Sigma Chemical Co., Japan) and zolantidine (Nakarai tesuku Co., Japan) were dissolved in saline, while terfenadine (Nakaraitesuku Co., Japan) was dissolved in saline containing 0.05% carboxymethylcellulose. All of the drugs were administered intraperitoneally at a dose of 10 mg/kg. The dose of 10 mg/kg was decided on the basis of our previous study where diphenhydramine, another H1-blocker, suppressed rotation-induced kaolin intake dose-dependently at an optimal dose of 10 mg/kg. Control animals were injected with the same volume of saline. Each drug or saline was administered 30 min before the second hypergravity load. Kaolin consumption on day 4 indicated the amount of kaolin consumed during 24 h after the first hypergravity load, whereas that on day 11 indicated the kaolin consumption during 24 h after the second load. Ratio of kaolin intake on day 11 and day 4 (day 11/day 4) was calculated and used as an index of the drug effect.

Effects of hypergravity on H1 receptor mRNA expression

Animals were exposed to 2 G hypergravity for 0, 2, 4, 6, or 12 h. Control animals were in the animal cage placed beside the centrifuge device for the same period but were not exposed to hypergravity. Each group was made up of six animals and a total of 60 animals were used.

Dissection of tissues and isolation of total RNA

Just after exposure to the hypergravity load, animals were sacrificed under an overdose anesthesia with pentobarbital. The hypothalamus, brainstem, and cerebral cortex were carefully dissected with a sharp

blade under microscopic guidance. The hypothalamus was dissected by cutting the brain at the level of optic chiasm and mammillary nucleus. From this block, only the ventral part of the thalamus was removed while the dorsal part was used as a cerebral cortex specimen after removal of the hippocampus and more ventral parts. The brainstem was dissected from the level of abducens nucleus to the solitary tract nucleus. Changes in H1R mRNA expression in the hypothalamus were investigated at the five time points (0, 2, 4, 6, and 12 h), whereas changes in the brainstem and the cerebral cortex were measured only after 4 h load of hypergravity.

Samples were frozen in RNAlater (Takara Biochemicals, Tokyo, Japan) and stored in a tube at −80°C until assayed. Total RNA was isolated using TRIzol reagent (Invitrogen Corp., Carlsbad, CA, USA) in accordance with the manufacturer's instructions. Samples were then homogenized using a Polytron (Model PT-K; Kinematica AG, Littau/Luzern, Switzerland) in 10 volumes of ice-cold TRIzol reagent until completely homogenized before the homogenates were mixed with chloroform and centrifuged at 15 000 rev/min for 15 min at 4°C. The aqueous phase containing RNA was transferred to a new tube and the RNA was precipitated by addition of isopropanol. Samples were incubated at room temperature for 5 min and centrifuged at 15 000 rev/min for 15 min at 4°C. The RNA pellet was washed with 70% ice-cold ethanol, air-dried, and then dissolved in 20 μl of diethlyrocarbonate-treated water. The purity and yield of total RNA were determined spectrophotometrically at 260 and 280 nm. The ratio of absorption (260:280 nm) of all preparations was 1.8–2.0.

Real-time quantitative reverse transcription polymerase chain reaction

RNA samples were reverse-transcribed to cDNA in a 47 μl reaction volume in the presence of first-strand buffer (375 mM KCl, 250 mM Tris-HCl, pH 8.3, at room temperature), 15 mM $MgCl_2$, 0.8 mM concentrations of each deoxyribonucleoside triphosphate (dNTP), 40 μM oligo (dT) primers, 0.004 units of RNase inhibitor, and 8 units of the reverse transcriptase. Samples were incubated at 37°C for 60 min before adding 2.35 μl of 2 N NaOH and then incubating again at 65 °C for 30 min. Subsequently, 14.3 μl of 1 M Tris-HCl, pH 8.0, were added and the samples were then heated at 95°C for 10 min and chilled to 4°C for 5 min. TaqMan primers and probe were designed using the Primer Express primer design software (Perkin Elmer Applied Biosystems, Foster City, CA, USA). The sequences of primers were as follows: sense primer, 5′-TAT GTG TCC GGG CTG CAC T-3′; antisense primer, 5′-CGC CAT GAT AAA ACC ACC CAA CTG-3′. The sequence of the probe was as follows: FAM-CCG AGA GCG GAA GGC AGC CA-TAMRA. To account for differences in starting material, rodent glyceraldehyde-3-phosphate dehydrogenase (GAPDH) primers and probe reagents from Applied Biosystems were used as recommended by the manufacturer. The transcripts were utilized for a 40 cycle, three-step polymerase chain reaction (PCR) using the GeneAmp5700 Sequence Detection System (Perkin Elmer Applied Biosystems) in 20 mM Tris, pH 8.4, 50 mM KCl, 3 mM $MgCl_2$, 200 μM dNTPs, 900 nM concentrations of each primer, and 0.25 units of platinum Taq. Amplicon size and reaction specificity were confirmed using agarose gel electrophoresis. The identity of the PCR products was verified by sequencing using a DNA thermocycler (4200L-1; Alolka, Tokyo, Japan).

The number of target copies in each sample was interpolated from its detection threshold (C_T) value using a purified PCR product standard curve included on each plate. Each PCR run included the four points of the standard curve (threefold serially diluted cDNA), a no-template control, the calibrator cDNA, and the unknown cDNAs. The measurements were calibrated using the calibrator included on each PCR plate. For the quantification of gene expression, we used GAPDH RNAs as the endogenous control. To determine whether the amplification products came exclusively from the RNA, a reverse transcriptase (RT)-negative reaction was run in which the enzyme was replaced by RNase-free water for each sample.

H1R mRNA in the hypothalamus was expressed as a percentage of that of the 0 h load. H1R mRNA in the brainstem and the cerebral cortex were evaluated after only 4 h load of hypergravity and expressed as a percentage of that of control animals that were in the animal cage placed beside the centrifuge device.

Effects of labyrinthectomy on hypergravity-induced H1 receptor mRNA expression

Under general anesthesia induced by sodium pentobarbital (50 mg/kg, i.p.), labyrinthectomy was performed in rats using an operating microscope. The tympanic membrane, malleus, and incus were removed by the retroauricular approach. The stapes crusa were fractured and then the stapes footplate was removed to open the oval window. A small opening was established by drilling the bony horizontal semicircular canal. After aspiration of labyrinth fluid from the oval window, the membranous

labyrinth was rinsed with 100% ethanol. Previous histological studies confirmed that the labyrinth was completely destroyed and that the lesion did not extend to the adjacent region such as ganglion cells [10]. The same procedure was repeated in the contralateral ear 14 days after the first operation. After a recovery period of 14 days, animals were exposed to 2 G hypergravity load for 4 h. Sham-operated rats received bilateral retroauricular incisions with an interval of 14 days and were then exposed to 2 G hypergravity load for 4 h.

Statistical analysis

Data are presented as mean ± SE. All p values were determined using one-way analysis of variance (ANOVA). Fisher's paired least significant difference test was used in the experiment for drug effects and Scheffe's F test in the experiment for H1 receptor mRNA expression. $p < 0.05$ was considered significant.

Results

Effects of histaminergic receptor blockers on kaolin intake induced by hypergravity load

Kaolin intake from day 1 to day 13 of each group is shown in Figure 1A. Rats did not take a significant amount of kaolin before hypergravity load (days 1–3, Figure 1A). However, kaolin intake in all of the groups increased after the first hypergravity load (day 4). The second hypergravity load was delivered 1 week after the first load and was preceded by the administration of the respective drugs. Accordingly, kaolin intake in the saline, terfenadine, and zolantidine groups on day 11 was increased compared with that of day 4, but it was decreased in the mepyramine group (Figure 1A). Indeed, kaolin intake of the saline group on day 11 was increased to 134.2% of the intake on day 4 in the same group. On the contrary, kaolin intake in the mepyramine group was decreased to 71.9% compared to that of day 4 in the same group. The ratio of kaolin intake (day 11/day 4) in this group was significantly lower than that of the saline group ($p < 0.05$, Figure 1B).

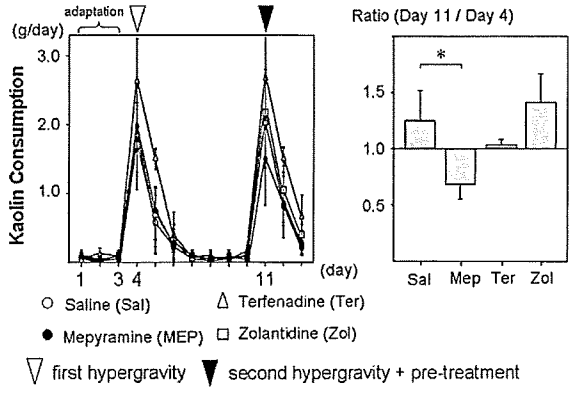

Figure 1. (A) Kaolin intake from day 1 to day 13 of each group. Kaolin intake in all of groups increased after the first hypergravity load (day 4). On day 11 after the second hypergravity load, which was preceded by drug administration, kaolin intake in the saline, terfenadine, and zolantidine groups was increased compared to that of day 4; however, it was decreased in the mepyramine group. (B) Ratio of kaolin intake on day 11 and day 4. Ratio of kaolin intake (day 11/day 4) in the mepyramine group was significantly lower compared with that of the saline group. *$p < 0.05$ vs saline group. Pretreatment with mepyramine suppressed the hypergravity-induced motion sickness.

H1 receptor mRNA expression in the hypothalamus, brainstem, and cerebral cortex after hypergravity load

Figure 2 shows the H1R mRNA expression in the hypothalamus of control rats (open column) and those exposed to hypergravity load for 0–12 h (closed column). Hypothalamic H1R mRNA expression remained unchanged in control animals, which were put into the centrifuge device but were not exposed to hypergravity load (open column). H1R mRNA expression in the hypothalamus gradually increased after hypergravity load (closed column). Hypothalamic H1R mRNA expression after 4 h load of hypergravity was 154.6% of the control animals. This difference reached a statistically significant level (4 h, open column vs 4 h, closed column, $p < 0.01$). It was also significantly higher compared with controls at 0 h (0 h, closed column vs 4 h, closed column, $p < 0.05$).

Figure 3 shows the H1R mRNA expression in the brainstem of animals exposed to hypergravity for 4 h

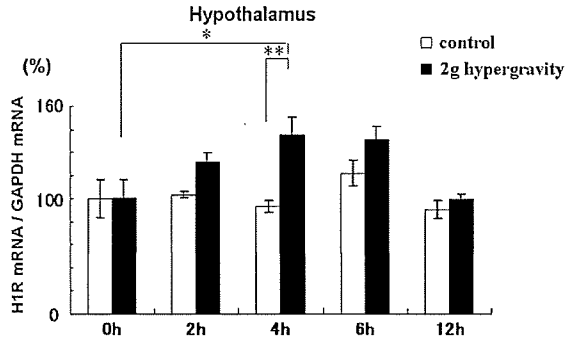

Figure 2. H1R mRNA expression in the hypothalamus of control rats (open column) and those exposed to hypergravity load for 0–12 h (closed column). Hypothalamic H1R mRNA expression after 4 h load of hypergravity was significantly higher than that of the control animals, which were in the animal cage placed beside the centrifuge device but not exposed to hypergravity for the same period (4 h, open column vs 4 h, closed column, **$p < 0.01$). It was also significantly higher compared with the controls at 0 h (0 h, closed column vs 4 h, closed column, *$p < 0.05$).

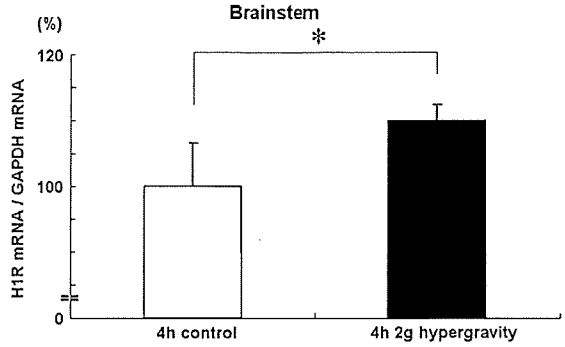

Figure 3. H1R mRNA expression in the brainstem. H1R mRNA expression in the brainstem of animals exposed to hypergravity for 4 h (closed column) was significantly higher than that of the control animals that were in the animal cage placed beside the centrifuge device but not exposed to hypergravity for the same period (open column). *$p < 0.05$ vs controls.

(closed column) or control animals that were in the animal cage placed beside the centrifuge device but not exposed to hypergravity during the same period (open column). H1R mRNA expression in the brainstem of animals exposed to hypergravity was significantly increased to 110.0% of the control animals ($p < 0.05$).

Figure 4 shows the H1R mRNA expression in the cerebral cortex of animals exposed to hypergravity for 4 h (closed column) or control animals that were in the animal cage placed beside the centrifuge device but not exposed to hypergravity during the same period (open column). No difference was noticed in H1R mRNA expression in the cerebral cortex between the controls and animals exposed to hypergravity.

Effects of labyrinthectomy on hypergravity-induced H1 receptor mRNA expression in the hypothalamus

H1R mRNA expression in the hypothalamus of the sham-operated rats exposed to hypergravity for 4 h was significantly increased to 118.2% of the bilaterally labyrinthectomized rats exposed to hypergravity for 4 h ($p < 0.05$) (Figure 5).

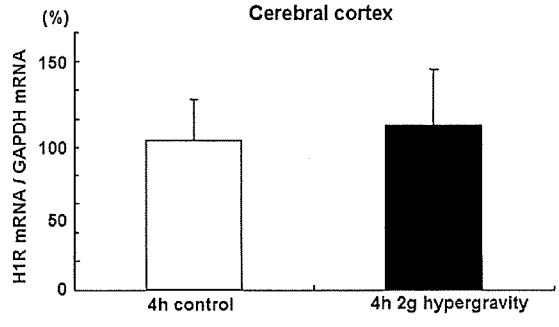

Figure 4. H1R mRNA expression in the cerebral cortex. There were no differences in H1R mRNA expression in the cerebral cortex between control animals and those exposed to hypergravity for 4 h.

Discussion

H1 and H2 receptors are the major post-synaptic histaminergic receptors in both peripheral and central tissues, although there are four subtypes of histamine receptors (H1–H4) [11]. H1 blockers are clinically effective in preventing motion sickness [2,3], suggesting that H1 receptors play an important role in the development of motion sickness. In our previous study, kaolin intake induced by double rotation was suppressed by diphenhydramine, which is less specific to H1 receptors with anticholinergic actions [12]. In the present study, an attempt was made to clarify which subtype of post-synaptic histaminergic receptors was responsible for the development of motion sickness. The hypergravity-induced kaolin intake was significantly suppressed by pretreatment with mepyramine but not with terfenadine or zolantidine. Both mepyramine and terfenadine are specific H1 receptor blockers; however, the latter does not penetrate the BBB, acting only on the peripheral tissues. On the other hand, zolantidine is an H2 receptor blocker that does cross the BBB [13]. Therefore, the present results indicate that the central H1 but not H2 or peripheral H1 receptors play a pivotal role in the development of motion sickness.

We reported in the previous study that histamine release from the hypothalamus in rats was increased by 2 G hypergravity load [14], suggesting that the

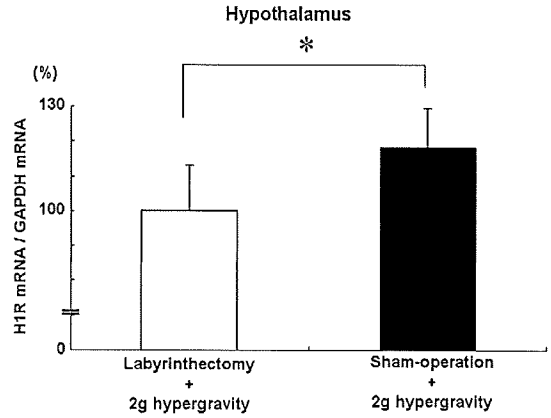

Figure 5. H1R mRNA expression in the hypothalamus of bilaterally labyrinthectomized rats (open column) and sham-operated rats (closed column) after hypergravity load for 4 h. H1R mRNA expression in the hypothalamus of the sham-operated rats was significantly increased in comparison with that of the bilaterally labyrinthectomized rats. *$p < 0.05$ vs bilaterally labyrinthectomized rats.

histaminergic neuron system was activated by hypergravity. Histaminergic neurons were located in the tuberomamillary nucleus in the posterior hypothalamus and their axons project both rostrally and caudally [15]. Therefore, it is suggested that the histaminergic activation is transmitted to the brain region related to the physiological and behavioral responses of motion sickness. Recently, it was reported that the stimulation of H1 receptor up-regulates the level of H1 receptor protein expression through augmentation of H1 receptor mRNA expression in HeLa cells and rats nasal mucosa [8,9]. In the present study, the expression of H1 receptor mRNA in the hypothalamus was significantly increased after a 4 h load of 2 G hypergravity in rats. However, the up-regulation of H1 receptor mRNA after hypergravity was not seen in bilaterally labyrinthectomized rats. These findings suggest that hypergravity stimulation induced the release of histamine from the hypothalamus through vestibular end-organs and the released histamine stimulated H1 receptors, leading to its up-regulation in the hypothalamus. Moreover, 2 G hypergravity load also significantly increased the expression of H1 receptor mRNA in the brainstem, but not in the cerebral cortex in rats. The brainstem includes the nuclei complex related to nausea and vomiting such as area postrema and nucleus of solitary tract, and was reported to contain histaminergic axon terminals [15]. Therefore, these findings suggest that hypergravity stimulation also induced the release of histamine from the brainstem and released histamine-stimulated H1 receptors on the nuclei complex related to nausea and vomiting, resulting in the development of motion sickness. The cerebral cortex is suggested not to be involved in the histaminergic post-synaptic events in the processes of motion sickness.

In fact, the hypothalamus has a role in various autonomic reactions such as cold sweating, pallor, and oliguria that characterize the motion sickness syndrome. Also, the brainstem contains nuclei complexes responsible for vomiting, which is a major symptom of motion sickness, such as the medullary reticular formation, nucleus tractus solitarii, and nucleus originis vagi. On the contrary, the cerebral cortex is undoubtedly involved in motion sickness in the modification of conditioned responses. Nevertheless, it is not essential for the development of motion sickness, because motion sickness can be induced in the decorticate human [16].

The up-regulation of H1 receptors in the hypothalamus and brainstem also indicates a post-synaptic amplification of H1 transmission in the development of motion sickness. The up-regulation of H1 receptors may contribute to the characteristic time course of motion sickness symptoms that develop gradually at first and then progressively more rapidly.

Conclusion

In conclusion, hypergravity-induced motion sickness in rats was prevented by BBB-penetrating H1 receptor blockers but not by non-BBB-penetrating H1 receptor blockers or H2 receptor blockers, suggesting that activation of H1 receptors in the brain is important for the development of motion sickness. The expression of H1 receptor mRNA was increased in the hypothalamus and brainstem, but not in the cerebral cortex after the hypergravity load in rats. It is suggested that histamine was released from the axon terminals in the hypothalamus and brainstem and released histamine activated the post-synaptic H1 receptors there, resulting in the development of motion sickness. The up-regulation of post-synaptic H1 receptors would amplify the histamine-mediated responses in motion sickness that develop gradually at first and then progressively more rapidly.

Acknowledgements

This study was supported by Grants-in Aid from the Ministry of Education, Science, Sports, and Culture of Japan and Health and Labor Science Grants in Japan. We thank Dr Kalubi Bukasa for his critical reading of the manuscript.

Declaration of interest: The authors report no conflicts of interest. The authors alone are responsible for the content and writing of the paper.

References

[1] Igarashi M. Role of the vestibular end organs in experimental motion sickness: a primate model. In: Crampton GH, ed. Motion and space sickness. Boca Raton, FL: CRC Press, 1990:43-8.

[2] Graybiel A, Wood CD, Knepton J, Hoche JP, Perkins GF. Human assay of anti-motion sickness drugs. Aviat Space Environ Med 1975;46:1107–18.

[3] Wood CD, Graybiel A. A theory of motion sickness based on pharmacological reaction. Clin Pharmacol Ther 1970;11: 621–9.

[4] Takeda N, Hasegawa S, Morita M, Horii A, Uno A, Yamatodani A, et al. Neuropharmacological mechanisms of emesis. I. Effects of anti-emetic drugs on motion- and apomorphine-induced pica in rats. Methods Find Exp Clin Pharmacol 1995;17:589–96.

[5] Takeda N, Hasegawa S, Morita M, Matsunaga T. Pica in rats is analogous to emesis: an animal model in emesis research. Pharmacol Biochem Behav 1993;45:817–21.

[6] Takeda N, Horii A, Uno A, Morita M, Mochizuki T, Yamatodani A, et al. A ground-based animal model of space adaptation syndrome. J Vestib Res 1996;6:403–9.

[7] Horii A, Takeda N, Matsunaga T, Yamatodani A, Mochizuki T, Okakura-Mochizuki K, et al. Effect of unilateral vestibular stimulation on histamine release from the hypothalamus of rats in vivo. J Neurophysiol 1933;70:1822–6.
[8] Das AK, Yoshimura S, Miyoshi R, Fujimoto K, Mizuguchi H, Dev S, et al. Stimulation of histamine H1 receptor up-regulates histamine H1 receptor itself through activation of receptor gene transcription. J Pharmacol Sci 2007;103:374–82.
[9] Kitamura Y, Miyoshi Y, Murata Y, Kalubi B, Fukui H, Takeda N. Effect of glucocorticoid on up-regulation of histamine H1 receptor mRNA in nasal mucosa of rats sensitized by toluene diisocynate. Acta Otolaryngol 2004; 124:1053–8.
[10] Horii A, Masumura C, Smith PF, Darlington CL, Kitahara T, Uno A, et al. Microarray analysis of gene expression in the rat vestibular nucleus complex following unilateral vestibular deafferentation. J Neurochem 2004;91:975–82.
[11] Haas H, Panula P. The role of histamine and tuberomammillary nucleus in the nervous system. Nat Rev Neurosci 2003;4:121–30.
[12] Morita M, Takeda N, Kubo T, Yamatodani A, Wada H, Matsunaga T. Effects of anti-motion sickness drugs on motion sickness in rats. ORL J Otolaryngol Relat Spec 1988;50:330–3.
[13] Calcutt CR, Ganellin CR, Griffiths R, Leigh BK, Maguire JP, Mitchell RC, et al. Zolantidine (SK&F 95282) is a potent selective brain-penetrating histamine H2-receptor antagonist. Br J Pharmacol 1988;93:69–78.
[14] Uno A, Takeda N, Horii A, Morita M, Kubo T, Yamamoto Y, et al. Histamine release from the hypothalamus induced by changes in gravity in rats and space motion sickness. Physiol Behav 1997;61:883–7.
[15] Wada H, Inagaki N, Yamatodani A, Watanabe T. Is the histaminergic neuron system a regulatory center for whole-brain activity? Trends Neurosci 1991;14:415–8.
[16] Doig RK, Wolf S, Wolff HS. Study of gastric function in a decorticate man with gastric fistula. Gastroenterology 1953; 23:40–4.

Acta Oto-Laryngologica, 2009; 129: 1044–1049

informa
healthcare

ORIGINAL ARTICLE

3D analysis of benign positional nystagmus due to cupulolithiasis in posterior semicircular canal

TAKAO IMAI[1,2], NORIAKI TAKEDA[3], MAHITO ITO[4], KAZUNORI SEKINE[3], GO SATO[3], YOSHIHIRO MIDOH[5], KOJI NAKAMAE[5] & TAKESHI KUBO[2]

[1]*Department of Otolaryngology, Osaka Seamen's Insurance Hospital, Osaka,* [2]*Department of Otolaryngology and Sensory Organ Surgery, Osaka University Graduate School of Medicine, Osaka,* [3]*Department of Otolaryngology, University of Tokushima School of Medicine, Tokushima,* [4]*Department of Otolaryngology, Kansai-Rosai Hospital, Hyogo and* [5]*Department of Information Systems Engineering, Osaka University Graduate School of Engineering, Osaka, Japan*

Abstract

Conclusions: The characteristic of both the vertical-torsional positional nystagmus with long time constant and its disappearance at the neutral head position could diagnose cupulolithiasis in posterior semicircular canal (PSCC) in the eight patients with the PSCC type of benign paroxysmal positional vertigo (P-BPPV). *Objective:* The aim of the study was to diagnose cupulolithiasis in patients with P-BPPV. *Patients and methods:* We used three-dimensional rotation axis analysis of nystagmus of the vertical-torsional positional nystagmus in 111 patients with P-BPPV and evaluated its time constant. We then examined whether the vertical-torsional positional nystagmus with long time constant disappeared at the neutral head position where the axis of the heavy cupula of the affected PSCC is aligned with gravity. *Results:* The first parameter showed a wide variation that could be divided into two groups: one lasting more than 40 s in 8 patients and another below 20 s in 103 patients. Since the time constant of the positional nystagmus induced by cupulolithiasis was much longer than that induced by canalolithiasis, this finding suggests that cupulolithiasis in the PSCC induced the vertical-torsional positional nystagmus with a long time constant in the group of eight patients. The vertical-torsional positional nystagmus disappeared in these patients at the neutral head position, where the axis of the cupula of affected PSCC aligned with gravity.

Keywords: *Cupulolithiasis, three-dimensional, rotation vector, posterior semicircular canal, infrared CCD camera, canalolithiasis*

Introduction

Recently, it has been recognized that the pathophysiology of benign paroxysmal positional vertigo (BPPV) is cupulolithiasis [1] or canalolithiasis [2,3] in either posterior semicircular canal (PSCC) or horizontal semicircular canal (HSCC). Patients with cupulolithiasis in HSCC show apogeotropic positional nystagmus [4–6], while those with canalolithiasis in HSCC show geotropic positional nystagmus [6,7]. Thus, the differential diagnosis of cupulolithiasis from canalolithiasis can be made by the direction of the positional nystagmus in patients with the HSCC type of BPPV (H-BPPV). On the other hand, in patients with the PSCC type of BPPV (P-BPPV), cupulolithiasis in PSCC induced the vertical-torsional positional nystagmus, in the same direction as that induced by canalolithiasis.

In a previous study, we found that the time constant of the positional nystagmus induced by cupulolithiasis was much longer than that induced by canalolithiasis in patients with H-BPPV [6]. Thus, their apogeotropic positional nystagmus lasted for a long time, while their geotropic positional nystagmus disappeared earlier. In addition, the positional nystagmus induced by cupulolithiasis was also characterized by its disappearance at the neutral head position where the axis of the heavy cupula of the affected ear was aligned with gravity [5].

Early disappearance of vertical-torsional positional nystagmus has been noticed in most patients

Correspondence: Takao Imai MD PhD, Department of Otolaryngology Osaka Seamen's Insurance Hospital, 1-8-30 Chikkou, Minato-ku, Osaka-shi, Osaka 552-0021, Japan. Tel: +81 6 6572 5721. Fax: +81 6 6573 2531. E-mail: imaitakao@hotmail.com

(Received 10 September 2008; accepted 20 October 2008)

ISSN 0001-6489 print/ISSN 1651-2251 online
DOI: 10.1080/00016480802566303

with P-BPPV, suggesting that their pathophysiology was canalolithiasis. In the present study, an attempt was made to diagnose cupulolithiasis in some patients with P-BPPV. For this purpose, we used the three-dimensional (3D) rotation axis analysis of nystagmus and examined the time constant of the vertical-torsional positional nystagmus in patients with P-BPPV. We then examined whether the vertical-torsional positional nystagmus with long time constant disappeared at the neutral head position where the axis of the heavy cupula of the affected PSCC is aligned with gravity.

Patients and methods

The study included 111 patients with P-BPPV (41 male, 70 female; 23–83 years old, average age 61 years). P-BPPV was diagnosed by the following criteria [3]: (i) a history of brief episodes of positional vertigo, (ii) a vertical-torsional paroxysmal positional nystagmus triggered by Dix-Hallpike (D-H) maneuver [8] or head rotation to either left or right in supine, (iii) no evidence of other neurologic or otologic diseases.

All positional nystagmus was recorded on videotape with an infrared CCD camera (*RealEyes*, Micromedical Technologies). The description of the eye movements in 3D was done using rotation vectors, which characterize the 3D eye position by a single rotation. The rotation vector was given by the axis of rotation, and its length was proportional to the size of the rotation. An eye position could be reached by rotating the eye from a reference position on a single axis. This eye position was represented by a vector along a single axis of which a length is proportional to the angle of the rotation. The reference position was defined as the position assumed by the eye when the subject was looking straight ahead with the head kept upright, while straight ahead was defined as looking at a target located horizontally in front of the eye [9]. The eye rotation vectors analysis method and its accuracy have already been described [10,11].

We converted the videotape images into 30 Hz digital images (640*480 dot) (*PCV-R63K*, Sony) and from these we reconstructed the space coordinates of the center of the pupil and an iris freckle. These coordinates (X, Y, Z) were defined so that the X-axis was parallel to the naso-occipital axis (positive forward), Y-axis parallel to the inter-aural axis (positive left), and Z-axis normal to the X-Y plane (positive upwards). X, Y, and Z components mainly reflect the roll, pitch, and yaw components, respectively. Because Euler angle is familiar, we used axis-angle representations [12,13]. Using this method, we have already reported the 3D analysis of positional nystagmus in BPPV patients [6,14,15]. In addition, we calculated the slow phase eye velocity (SPEV) ω around X, Y, and Z axes [9] and extracted the slow phase data from nystagmic eye movement data by using the method (patent applied for) based on a fuzzy set approach [16,17]. Using the least squares method, SPEV in X component against time was approximated exponentially. Finally, the time constant was calculated as the reciprocal of the coefficient of time [18].

Results

In the present study, P-BPPV was diagnosed based on the criteria defined for the above-mentioned 111 patients in addition to the 3D analysis of their vertical-torsional positional nystagmus. We calculated SPEV in the X component of their positional nystagmus triggered by D-H maneuver or head rotation to either left or right in supine and evaluated its time constant. Time constants were divided into two groups: one was below 20 s in 103 patients and another was above 40 s in 8 patients (Figure 1).

Figures 2–4 show changes in eye position and SPEV in X, Y, and Z components of the positional nystagmus in two representative patients: patient A with short time constant under 20 s, and patient B with long time constant over 40 s. The right side was the affected side in both patients. After right D-H maneuver, the positional nystagmus soon disappeared in patient A (Figure 2A) and SPEV quickly declined in X and Y components (Figure 3A). The time constant of SPEV in X component of her positional nystagmus was 5.48 s, indicating that patient A had canalolithiasis in her right PSCC.

On the contrary, the positional nystagmus in patient B showing P-BPPV persisted for more than 1 min when his head was rotated to the right in supine (Figure 2B) while the SPEV in X and Y components gradually declined (Figure 3B). The

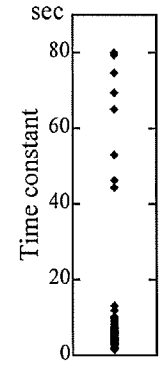

Figure 1. Time constants of all patients. The time constant was divided into two groups: one lasting <20 s and the other >40 s.

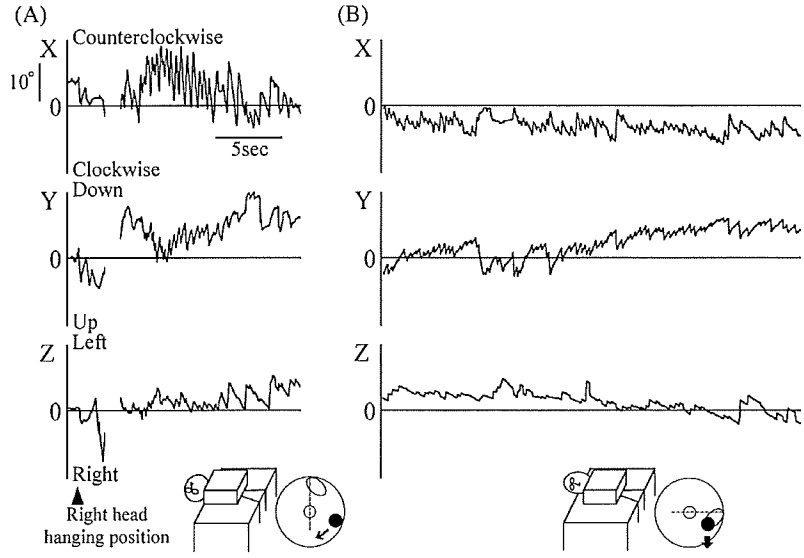

Figure 2. Eye positions in X, Y, and Z components of nystagmus in patients A and B. (A) Right D-H maneuver in patient A. (B) Right head rotated position in supine in patient B. Inserted figures show their head position and their right PSCC with canalolithiasis (●) in (A) and cupulolithiais (●) in (B). The direction of the arrow in the inserted PSCC figure in (A) shows the direction of the movement of the canalolithiasis. The direction of the arrow around the inserted PSCC figure in (B) shows the direction of gravity. The dotted line in the right PSCC shows the position of cupula when it is not deflected.

clockwise SPEV in X component of the positional nystagmus reached a maximum velocity of 9.37°/s (filled triangle in Figure 3B), which declined exponentially. The SPEV time constant in X component of her positional nystagmus was 44.4 s. In the same patient, the positional nystagmus disappeared (Figure 4A, shown by open triangle in Figure 3B) in right head hanging position with further extension of the neck.

Moreover, patient B showed direction-changing vertical-torsional positional nystagmus. In left head hanging position, she showed a positional nystagmus with clockwise fast phase in X component and downward fast phase in Y component of the eye

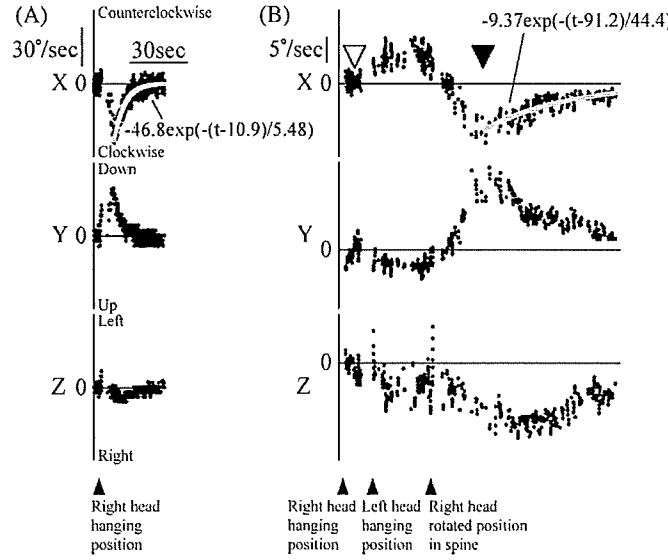

Figure 3. SPEV in X, Y, and Z components of nystagmus: (A) patient A; (B) patient B. Upper, middle, and lower recordings are X, Y, and Z components of SPEV, respectively. The time constant of positional nystagmus in patient B (44.4 s) is much longer than that in patient A (5.48 s).

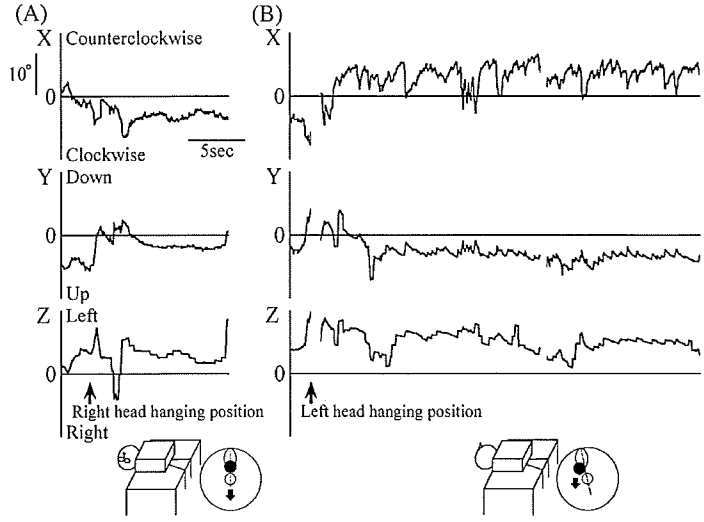

Figure 4. Eye position in X, Y, and Z components of nystagmus in patient B. (A) Right D-H maneuver. (B) Left D-H maneuver. Inserted figures show her head position and her right PSCC with cupulolithiais (●). The direction of the arrow around the inserted PSCC figures shows the direction of gravity. The dotted line in right PSCC shows the position of the cupula when it is not deflected.

position (Figure 4B), as well as a counterclockwise SPEV in X component and an upward SPEV in Y component (Figure 3B). Rotation of the head to the right in supine caused the inversion of all these parameters in the X and Y components.

Finally, in patient B, SPEVs of the axis angles of positional nystagmus shown in Figure 3B were plotted on XY, XZ, and YZ planes (Figure 5). Accordingly, clockwise SPEV in X component and downward SPEV in Y component were in line with the axis perpendicular to the right PSCC plane (Rp) [19]. Conversely, counterclockwise SPEV in X component and upward SPEV in Y component were in line with the axis perpendicular to the left anterior semicircular canal (ASCC) plane (La) [19].

Discussion

In the present study, we three-dimensionally analyzed the vertical-torsional positional nystagmus in 111 patients with P-BPPV and evaluated their time

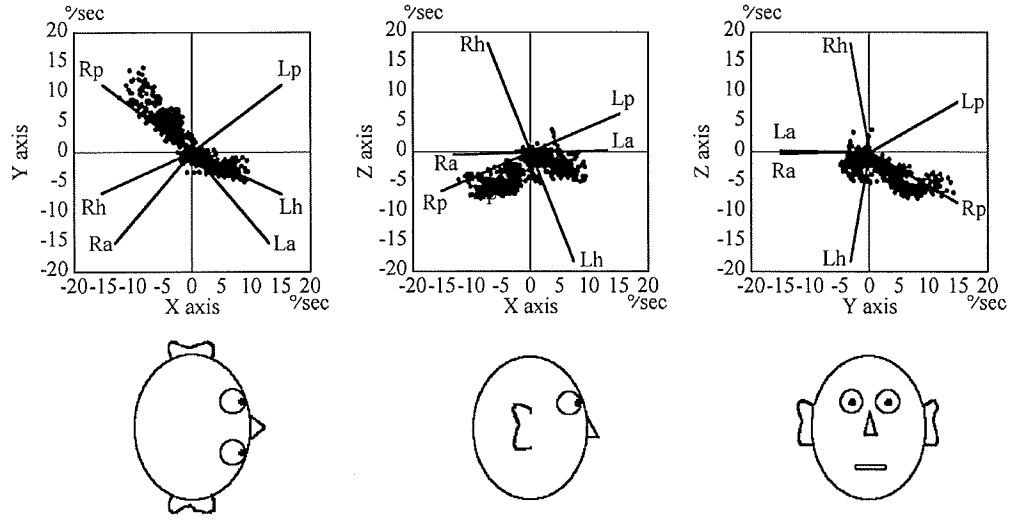

Figure 5. Three-dimensional plotting of the axis angle of SPEV that is shown in Figure 3B. Ra, axis perpendicular to the plane of the right ASCC; Rh, axis perpendicular to the plane of the right HSCC; Rp, axis perpendicular to the plane of the right PSCC; La, axis perpendicular to the plane of the left ASCC; Lh, axis perpendicular to the plane of the left HSCC; Lp, axis perpendicular to the plane of the left PSCC [19].

constant. The time constant of their positional nystagmus varied widely, but could be divided into two groups: one lasting more than 40 s in 8 patients and another less than 20 s in 103 patients (Figure 1). In a previous study, we found that the time constant of the positional nystagmus induced by cupulolithiasis was much longer than that induced by canalolithiasis in patients with H-BPPV [6]. This finding suggests that cupulolithiasis in PSCC induces the vertical-torsional positional nystagmus with a long time constant (>40 s) in 8 patients, while canalolithiasis in PSCC induces with short time constant (<20 s) in 103 patients.

In patients with H-BPPV, cupulolithiasis-induced apogeotropic positional nystagmus was characterized by its disappearance at the neutral head position where the axis of the heavy cupula of the affected ear was aligned with gravity [5]. We then examined whether the vertical-torsional positional nystagmus with long time constant disappeared at a specific head position in eight patients because the existence of the neutral head position is characteristic of cupulolithiasis. The positional nystagmus in patient B disappeared in right head hanging position with further extension of the neck (Figure 4A, open triangle in Figure 3B), when the axis of the cupula of right PSCC was aligned with gravity (inserted figure in Figure 4A). The positional nystagmus with long time constant in the other seven patients disappeared in the same head position (data not shown). Therefore, the observation of disappearance of a vertical-torsional positional nystagmus when the head is brought to the neutral head position suggests a cupulolithiasis in the PSCC of eight patients.

Furthermore, we examined whether the vertical-torsional positional nystagmus showed a direction-changing characteristic in these eight patients. Patient B showed positional nystagmus with a counterclockwise SPEV in X component and an upward SPEV in Y component (Figure 3B and 4B) in left head hanging position when the heavy cupula was bent in ampullopetal direction by gravity (inserted figure in Figure 4B). Conversely, in a right head rotation in supine when the cupula was bent in an ampullofugal direction by gravity (inserted figure in Figure 2B), patient B showed a positional nystagmus with clockwise SPEV in X the component, and a downward SPEV in Y component (Figure 2B, filled triangle in Figure 3B). Thus, direction-changing vertical-torsional positional nystagmus shown by patient B in various head positions can be explained by cupulolithiasis in the right PSCC. The other seven patients showed the same direction-changing vertical-torsional positional nystagmus (data not shown).

Finally, SPEVs of the axis angle of direction-changing vertical-torsional positional nystagmus in patient B were analyzed and plotted on XY, XZ, and YZ planes (Figure 5). Clockwise SPEV of the axis angle of positional nystagmus in X component and downward SPEV in Y component were in line with the axis perpendicular to the right PSCC plane (Rp). Conversely, counterclockwise SPEV in X component and upward SPEV in Y component were in line with the axis perpendicular to the left ASCC plane (La). This finding corroborates that of a previous report, which showed that the ampullofugal stimulation of the PSCC induced nystagmus around the axis perpendicular to ipsilateral PSCC, and the ampullopetal stimulation of PSCC induced nystagmus around the axis perpendicular to contralateral ASCC [20]. The direction-changing vertical-torsional positional nystagmus in patient B in left head hanging and right head rotated positions, which was suppressed by the neutral head position, can be explained by the flexion of the cupula attached with cupulolithiasis in PSCC. SPEVs of the axis angle of direction-changing vertical-torsional nystagmus in the other seven patients were in line with the axis perpendicular to ipsilateral PSCC and the axis perpendicular to contralateral ASCC (data not shown).

In the present study, we diagnosed P-BPPV in 111 patients and in 8 of them found a vertical-torsional positional nystagmus with a long time constant (>40 s). This nystagmus disappeared at the neutral head position. They also showed a direction-changing vertical-torsional positional nystagmus in left and right head rotated positions in supine, which was suppressed by the neutral head position. Finally, the axis angles of their positional nystagmus were in line with ipsilateral PSCC and contralateral ASCC. All these findings suggest that the development of a cupulolithiasis in the PSCC may be the underlying cause of BPPV in a small portion of patients with this condition.

Declaration of interest: The authors report no conflicts of interest. The authors alone are responsible for the content and writing of the paper.

References

[1] Schuknecht HF. Cupulolithiasis. Arch Otorhinolaryngol 1969;90:765–78.
[2] Epley JM. The canalithi repositioning procedure: for treatment of benign paroxysmal positional vertigo. Otolaryngol Head Neck Surg 1992;107:399–404.
[3] Brandt T. Benign paroxysmal positioning vertigo. In: Brandt T, ed. Vertigo: its multisensory syndromes, 2nd edn. London: Springer-Verlag, 1999:251–83.

[4] Casani A, Giovanni V, Bruno F, Luigi GP. Positional vertigo and ageotropic bi-directional nystagmus. Laryngoscope 1997;107:807–13.
[5] Bisdorff AR, Debatisse D. Localizing signs in positional vertigo due to lateral canal cupulolithiasis. Neurology 2001;57:1085–8.
[6] Imai T, Takeda N, Sato G, Sekine K, Ito M, Nakamae K, et al. Changes in slow phase eye velocity and time constant of positional nystagmus at transform from cupulolithiasis to canalolithiasis. Acta Otolaryngol 2008;128:22–8.
[7] McClure JA. Horizontal canal BPV. J Otolaryngol 1985;14:30–5.
[8] Dix MR, Hallpike CS. Pathology, symptomatology and diagnosis of certain disorders of the vestibular system. Proc R Soc Med 1952;45:341–54.
[9] Haslwanter T. Mathematics of three-dimensional eye rotations. Vision Res 1995;35:1727–39.
[10] Imai T, Takada N, Morita M, Koizuka I, Kubo T, Miura K, et al. Rotation vector analysis of eye movement in three dimensions with an infrared CCD camera. Acta Otolaryngol 1999;119:24–8.
[11] Imai T, Sekine K, Hattori K, Takeda N, Koizuka I, Nakamae K, et al. Comparing the accuracy of video-oculography and the scleral search coil system in human eye movement analysis. Auris Nasus Larynx 2005;32:3–9.
[12] Schnabolk C, Raphan T. Modeling three dimensional velocity-to-position transformation in oculomotor control. J Neurophysiol 1994;71:623–38.
[13] Raphan T. Modeling control of eye orientation in three dimensions. I. Role of muscle pulleys in determining saccadic trajectory. J Neurophysiol 1998;79:2653–67.
[14] Imai T, Takeda N, Ito M, Nakamae K, Sakae H, Fujioka H, et al. Three-dimensional analysis of benign paroxysmal positional nystagmus in a patient with anterior semicircular canal variant. Otol Neurotol 2006;27:362–6.
[15] Imai T, Takeda N, Sato G, Sekine K, Ito M, Nakamae K, et al. Differential diagnosis of true and pseudo-bilateral benign positional nystagmus. Acta Otolaryngol 2008;128:151–8.
[16] Naoi K, Nakamae K, Fujioka H, Imai T, Sekine K, Takeda N, et al. Three-dimensional eye movement simulator extracting instantaneous eye movement rotation axes, the plane formed by rotation axes, and innervations for eye muscles. IEICE Trans Inf Syst 2003;11:2452–62.
[17] Arzi M, Mignin M. A fuzzy set theoretical approach to automatic analysis of nystagmic eye movements. IEEE Trans Biomed Eng 1987;36:954–63.
[18] Brantberg K, Fransson P-A, Bergenius J, Tribukait A. Tilt suppression, OKAN, and head-shaking nystagmus at long-term follow-up after unilateral vestibular neurectomy. J Vestib Res 1996;4:235–41.
[19] Blanks RHI, Curthous IS, Markham CH. Planar relationships of the semicircular canals in man. Acta Otolaryngol 1975;80:185–96.
[20] Fetter M, Aw S, Haslwanter T, Heimberger J, Dichgans J. Three-dimensional eye movement analysis during caloric stimulation used to test vertical semicircular canal function. Am J Otol 1998;19:180–7.

Neuroscience 165 (2010) 1323–1332

BEHAVIORAL ASSESSMENT AND IDENTIFICATION OF A MOLECULAR MARKER IN A SALICYLATE-INDUCED TINNITUS IN RATS

K. KIZAWA, T. KITAHARA,* A. HORII, C. MAEKAWA, T. KURAMASU, T. KAWASHIMA, S. NISHIIKE, K. DOI AND H. INOHARA

Department of Otolaryngology-Head and Neck Surgery, Osaka University, School of Medicine, 2-2 Yamada-oka, Suita-City, Osaka 565-0871, Japan

Abstract—Tinnitus is a non-observable phantom sensation. As such, it is a difficult condition to investigate and, to date, no effective treatment has been developed. To approach this phantom sensation, we aimed to develop a rat behavioral model of tinnitus using salicylate, an active component of aspirin known to induce tinnitus. We also aimed to establish a molecular marker of tinnitus by assessing the expression of transient receptor potential cation channel superfamily V-1 (TRPV1) in the rat auditory pathway during salicylate-induced tinnitus. Animals were trained to perform "an active avoidance task": animals were conditioned by electrical footshock to move to the other side of the conditioning box when hearing a sound. Animals received a single injection of saline or salicylate (400 mg/kg i.p.) and false positive responses were measured 2 h after injection as the number of movements during a silent period. The number of responses in salicylate-treated animals was highest when the conditioned stimulus was 60 dB sound pressure level (SPL) and 16 kHz. This indicates that animals could feel tinnitus 2 h after salicylate injection, equivalent to that induced by 60 dB SPL and 16 kHz. By means of real-time PCR and western blot analysis, TRPV1 expression was significantly upregulated in spiral ganglion cells 2 h after salicylate injection and this upregulation together with the increase in the number of false positive responses was significantly suppressed by capsazepine (10 mg/kg i.p.), a specific antagonist of TRPV1. This suggests that salicylate could induce tinnitus through activation of TRPV1 in the rat auditory pathway.

Key words: animal model, TRPV1, spiral ganglion, dorsal cochlea nucleus.

Many people have experienced a sensation of ringing in their ears when no external sound is present. Typically, this sensation of tinnitus is associated with a reversible cause and subsides over a period of time ranging from a few seconds to a few days. However, in 5–15% of the general population, the tinnitus is unremitting (Heller, 2003). Chronic tinnitus is more prevalent among seniors (12% after the age of 60) than in young adults (5% in the age group 20–30), but can occur at any age. In 1–3% of the general population, tinnitus is perceived as loud enough to affect the quality of life (Eggermont and Roberts, 2004). However, no effective therapeutic strategy for such intractable tinnitus has been established.

There are at least two obvious reasons why it is still so hard for clinicians to treat intractable tinnitus. One reason is that, since Jastreboff and Sasaki (1994) proposed an animal behavioral model of tinnitus based on an active avoidance task of drinking water with electrical footshock, better feasibility of the model has been discussed. The first purpose of the present study was, therefore, to develop a rat behavioral model to enable the objective evaluation of tinnitus. Salicylate, an active component of aspirin, is well known to induce an acute and transient type of tinnitus (Cazals, 2000; Eggermont and Roberts, 2004). According to the recent good work of climbing a pole with electrical footshock by Guitton et al. (2003), our model using salicylate was developed with modifications of a much easier active avoidance task. These previous and present tinnitus models will be addressed again in the first paragraph in Discussion.

The other reason is that the molecular mechanism of tinnitus generation in the auditory pathway has not been clarified yet. The second purpose of the present study was, therefore, to identify molecular markers to understand the molecular mechanism of salicylate-induced tinnitus in the rat auditory pathway. Salicylate inhibits cyclo-oxygenase activity (Christie et al., 1998) and cyclo-oxygenase inhibition leads to the *in vitro* activation of a nociceptive receptor transient receptor potential cation channel superfamily V-1 (TRPV1) (Fosslien, 1998; Hwang et al., 2000; Caterina et al., 1997; Benham et al., 2003). TRPV1 is located in the mouse inner ear ganglia and is upregulated *in vivo* after noxious challenges of kanamycin (Kitahara et al., 2005a). Furthermore, cochlear background activity is increased by inner ear perfusion of capsaicin, a TRPV1 agonist and is suppressed by capsazepine, a TRPV1 specific antagonist (Zhou et al., 2006). We examined changes in mRNA and protein levels of TRPV1 in the salicylate-treated rat auditory pathway. Although salicylate-induced tinnitus is acute and transient, we believe that by elucidating the molecular mechanism of salicylate-induced tinnitus we can provide insight into chronic intractable tinnitus.

*Corresponding author. Tel: +081-6-6879-3951; fax: +81-6-6879-3959.
E-mail address: tkitahara@ent.med.osaka-u.ac.jp (T. Kitahara).
Abbreviations: ABR, auditory brainstem response; BRCx, brain cortex; B2m, beta-2 microglobulin; CT, cycle threshold; DCN, dorsal cochlear nucleus; DMSO, dimethyl sulfoxide; RT, room temperature; SG, spiral ganglion; SPL, sound pressure level; TRPV1, transient receptor potential cation channel superfamily V-1.

0306-4522/10 $ - see front matter
doi:10.1016/j.neuroscience.2009.11.048

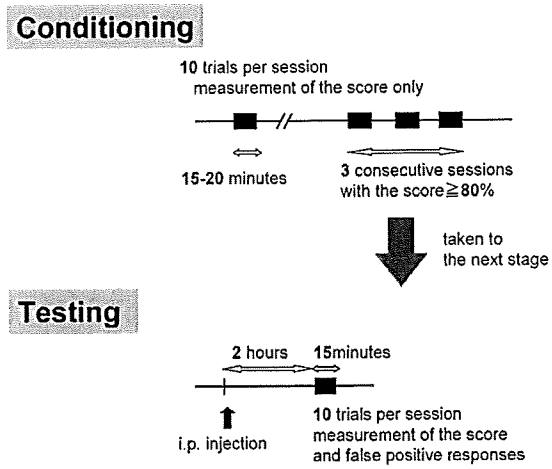

Fig. 1. Schematic representation of the behavioral protocol. In "conditioning," animals were conditioned to move in response to a sound stimulation. The conditioning procedure requires up to seven sessions lasting 15–20 min. When conditioned (criterion, three consecutive sessions with an active avoidance score ≥80%), animals were taken to the next stage, "testing" (day 0). The "testing" behavioral protocol consisted of a daily measurement (on four consecutive days, days 1–4) of the correct responses to sound (active avoidance score) and moves during inter-trial periods (false positive responses) in a 15 min session. Saline or salicylate was injected daily 2 h before the testing session.

EXPERIMENTAL PROCEDURES

Experimental procedures involving animals were performed according to animal ethical guidelines and were approved by Osaka University, School of Medicine (certificate number: 0755). All efforts were made to minimize the suffering to animals and to limit the number of animals used. A total of 99 male Wistar rats (Japan SLC, Hamamatsu, Shizuoka, Japan), weighting between 150 and 200 g, were used. Animals were individually housed in a temperature-controlled room on a constant 12 h light/dark cycle. All behavioral tests were conducted during the animals' activity period (dark phase) at approximately the same time each day. Food and tap water were available throughout the experiments.

Behavioral assessment

Animals were trained to perform "an active avoidance task," according to the protocol of Guitton et al. (2003) (Fig. 1). Both "conditioning" and "testing" were performed in a conditioning box that had an electrified floor, which was divided in two by a low wall, 3 cm high. The conditioning box was in a soundproof room. A 5 s pure tone sound was used as the "conditioned stimulus" and a 3.7 mA electrical footshock was given for a maximum of 30 s as the "unconditioned stimulus." The interval between conditioned and unconditioned stimuli was 1 s. The footshock was stopped when animals correctly escaped from the unconditioned shock to the opposite side of the cage. The inter-trial interval or silent period was at least 1 min. The level of performance over 10 trials, or "active avoidance score," was assessed by the ratio of how many times the rat moved correctly in response to the conditioned sound. In the "conditioning" stage, animals were considered to be conditioned when the active avoidance score reached at least 80% in three consecutive sessions. When conditioned, animals were taken to the next "testing" stage (day 0).

Testing was performed once daily for 4 days, at the same time each day (day 1–4). Animals received a single daily injection of saline or sodium salicylate (400 mg/kg i.p.) (Sigma, St. Louis, MO, USA) for 3 days (day 1–3), according to the previous reports of Jastreboff and Sasaki (1986); Rüttiger et al. (2003) and Im et al. (2007). Injections were performed 2 h before behavioral measurements. On the fourth day, they received no treatment. The behavioral protocol consisted of a daily measurement of the active avoidance score and of false positive responses. The "false positive responses" represent the number of movements to the opposite side of the cage during the inter-trial interval, when there was no sound. Trials were randomized and electric footshocks were presented only if animals didn't move in response to sounds. Whatever the results of the active avoidance score and false positive responses were, each session included 10 trials and lasted 15 min. Both the active avoidance score and false positive responses were measured in the same session.

The most appropriate conditioned stimulus was determined by the following pilot experiments. Animals were divided into four groups (n=6 in each group) according to conditioned stimuli of 4, 10, 16 or 40 kHz (60 dB sound pressure level (SPL)), and false positive responses were measured on the third day after salicylate injection. Animals were also divided into three groups (n=6 in each group) according to conditioned stimuli of 20, 60 or 80 dB SPL (16 kHz) and false positive responses were measured as above.

Auditory brainstem response (ABR) recording

The ABR was measured with a Neuropack-4 (Nihon Koden Co., Shinjuku, Tokyo, Japan). The active platinum electrode was inserted at the vertex, and reference electrodes at both pinnae of the ears. Binaural, open fielded stimuli of click were generated through a TDH-49 headphone attached to the animal's ears. The rat ABR consisted of a series of III to V vertex-positive peaks within the first 6 ms from the onset of the stimulus, and they were called I to V. The III wave was detected at the lowest stimulus intensity, so the threshold was defined as the lowest stimulus intensity to elicit a reliable III wave.

Hematoxylin and eosin staining

Serial inner ear sections from saline controls and salicylate-treated rats were stained with hematoxylin and eosin to determine if salicylate treatment caused any overt damage to the inner ear. Morphological structures in the organ of Corti and the spiral ganglion (SG) were microscopically observed.

Analysis of mRNA levels

Animals were divided into five groups: a saline i.p. injection control group, a 2 h post-salicylate i.p. injection group, a 12 h post-salicylate injection group, a 24 h post-salicylate injection group, and a 72 h post-salicylate injection group (n=6 in each group).

The procedures of tissue preparation for real-time PCR have already been described in our previous papers (Kitahara et al., 2005a,b). Animals were deeply anesthetized with pentobarbital and the SG, dorsal cochlear nucleus (DCN) and brain cortex (BRCx) were immediately dissected under a stereomicroscope in chilled buffered saline and then frozen in dry ice powder. The DCN region is thought to be one of the main structures involved in tinnitus (Eggermont and Roberts, 2004) and it was carefully dissected according to the coordinates of the Paxinos and Watson brain atlas; rostral coordinate, bregma: −10.52 mm, and caudal coordinate, bregma: −11.60 mm (Paxinos and Watson, 1986). The BRCx region does not include the auditory cortex. Total RNA was extracted using an RNeasy Mini Kit (Qiagen, Venlo, Netherlands) according to the manufacturer's instructions.

PCR was performed using oligonucleotide primers for TRPV1 (Takara Bio Inc., Otsu, Shiga, Japan) and beta-2 microglobulin (B2m) (Takara), as shown in Table 1, and products were quantified by SYBR Green PCR reagents (Applied Biosystems, Foster City, CA, USA). B2m was assayed as a control housekeeping gene. The PCR mixture included 10 μl of 2× SYBR Premix Taq,

Table 1. Gene-specific primers for PCR of rat transient receptor potential cation channel superfamily V type 1 (TRPV1) and β-2 microglobulin (B2m)

TRPV1 (accession no. NM_031982)
Forward primer 5′-ACTCCTGACGGCAAGGATGAC-3′
Reverse primer 5′-ACCCACATTGGTGTTCCAGGTAG-3′
Estimated size 81 bp
B2m (accession no. NM_012512)
Forward primer 5′-CCTGGCTCACACACTGAATTCACAC-3′
Reverse primer 5′-AACCGGATCTGGAGTTAAACTGGTC-3′
Estimated size 163 bp

0.8 μl of each gene-specific primer (5 μM), 6.8 μl of dH2O, 0.4 μl of 50× ROX Reference Dye and 2 μl of cDNA (250 ng) in a final volume of 20 μl. The conditions used were 95 °C for 10 s, 40 cycles at 95 °C for 5 s and 60 °C for 30 s, 95 °C for 15 s, 60 °C for 1 min and 95 °C for 15 s. The amplification plots from fluorescent emission data collected during PCR were constructed using the ABI7900 model software (Applied Biosystems).

The number of PCR cycles was recorded until the fluorescence intensity exceeded the pre-determined threshold. The quantification of the initial amounts of template molecules relied on this number of PCR cycles, which is termed the cycle threshold (CT). The dCT represents the CT of the target gene normalized to the rat endogenous B2m ($dCT=CT_{target}-CT_{B2m}$). Relative quantification of the mRNA levels of target genes (=fold range) was calculated using the 2^{-ddCT} method, where $ddCT=(CT_{target}-CT_{B2m})A-(CT_{target}-CT_{B2m})B$ (Schmittgen et al., 2000). For example, changes in gene expression of TRPV1 among groups CONT, SA2H, SA12H, SA24H and SA72H ($GROUP_x$) within each region were quantified as the fold range: 2^{-ddCT} ($ddCT=(CT_{TRPV1}-CT_{B2m})_{GROUPx}-(CT_{TRPV1}-CT_{B2m})_{CONT}$).

Protein examination

TRPV1 protein levels were assayed using standard western blotting techniques (Kitahara et al., 2005a,b). Briefly, tissues of each region (SG, DCN, BRCx) were obtained from a saline i.p. injection control group, a 2 h post-salicylate i.p. injection group and a 24 h post-salicylate injection group ($n=8$ in each group) through the same procedure for real-time PCR in the present study. Then, the tissues were added to lysis buffer (1% NP-40, 150 mM NaCl, 1 mM EDTA, 10 mM PBS (pH 7.4), 0.25 mM DTT, 1 mM phenylmethylsulfonyl fluoride, 10 μg/ml aprotinin, 10 μg/ml leupeptin) and homogenized gently on ice using a Polytron tissue homogenizer (Brinkmann Instruments, Westbury, NY, USA). The samples were boiled for 1 min, transferred to clean Eppendorf tubes on ice and centrifuged at 10,000 g for 30 min. Supernatant was transferred to clean tubes, and protein concentration was determined using a protein assay kit (Pierce, Rockford, IL, USA). The protein extracts (20 μg for each lane) were subjected to 12% SDS-polyacrylamide gel electrophoresis and transferred to nitrocellulose filters (Amersham Biosciences, Piscataway, NJ, USA) at 500 mA for 1 h. The filters were pre-blocked in 0.1 M PBS containing 0.2% Tween 20 and 5% non-fat dried milk for 3 h at room temperature (RT), probed overnight with TRPV1 primary antibody (anti-rabbit polyclonal; diluted 1:1000; Alpha Diagnostic International, San Antonio, TX, USA) and then washed with Blotto solution (50 mM Tris (pH 7.4), 0.9% NaCl, 0.5% Tween 20) for 1 h. Filters were then incubated with HRP-conjugated secondary antibody (Dako, Carpenteria, CA, USA) for 1 h and washed with Blotto solution for 1 h. Protein bands were visualized using Supersignal Ultra chemiluminescence substrate (Pierce), assessed on ECL film (Amersham Biosciences) and quantified by laser densitometry (Quantity One Software, Bio-Rad Lab, Hercules, CA, USA). The density of staining with anti-β actin monoclonal antibody (Oncogene Research Products, Boston, MA, USA: diluted 1:500) was used to normalize the TRPV1 densitometric determination of each sample.

Tissue preparation procedures for immunohistochemistry have already been described in our previous papers (Kitahara et al., 2005a,b). Temporal bones were obtained from two adult male rats from each of a saline i.p. injection control group and a 2 h post-salicylate i.p. injection group. The animals were euthanized with sodium pentobarbital (100 mg/kg i.p.) and perfused transcardially with 0.1 M PBS, followed by paraformaldehyde-lysine-periodate fixative. Temporal bones were post-fixed in 4% paraformaldehyde for 24 h at RT, decalcified in 10% formic acid, neutralized overnight in 5% sodium sulfate, infiltrated with OCT compound and sectioned on a cryostat at 5 μm in a plane that produces mid-modiolar sections. The sections were thaw mounted on slides. The 5 μm cryostat sections were incubated sequentially in the following solutions at RT: 0.1% TritonX-100 and 2% bovine serum albumin (BSA) in 0.1 M PBS for 2 h; antisera against TRPV1 (anti-rabbit polyclonal; diluted 1:1000; Alpha Diagnostic International) in the above solution for 48 h; 0.1 M PBS for 15 min; biotinylated goat anti-rabbit IgG (diluted 1:250; Vector Laboratories, Burlingame, CA, USA) in 2% BSA in 0.1 M PBS for 24 h; 0.1 M PBS for 15 min; Vectastain ABC reagent (Vector Laboratories) for 1 h; 0.1 M PBS for 15 min; 5 mg/ml diaminobenzidine tetrahydrochloride (DAB)/0.01% H_2O_2 in 0.05 M Tris buffer for 5 min. Sections were then examined under a light microscope. For negative controls, primary antibodies were either pre-absorbed with each control peptide (1:50) or the primary antibody was omitted.

Antagonist treatment

To elucidate the direct involvement of TRPV1 in the mechanism of tinnitus generation, a specific antagonist of TRPV1, capsazepine (Sigma) and its vehicle, 50% dimetyl sulfoxide (DMSO) (Sigma) were used. Group I was a saline+DMSO group, group II was a salicylate+DMSO group, group III was a salicylate+capsazepine group and group IV was a saline+capsazepine group. DMSO or capsazepine was administrated 0.5 h after the first injection of saline or salicylate. Effects of capsazepine within the dose range of 0–10 mg/kg (De Schepper et al., 2008) were evaluated behaviorally by counting false positive responses (cf. 2.1 in Experimental Procedures) and morphologically by real-time PCR (cf. 2.3 in Experimental Procedures).

Statistical analysis

In the present paper, the statistical significance of changes among groups was analyzed using one-way ANOVA with Bonferroni *t*-test except for capsazepine treatment. Two-way ANOVA with Bonferroni *t*-test was used to test the hypotheses that salicylate effect is blocked by capsazepine. All the data were presented as mean±SE and *P*-values under 0.05 were considered significant (SPSS Inc., Chicago, IL, USA).

RESULTS

Behavioral assessment

In pilot experiments, animals were divided into four groups ($n=6$ in each group) according to conditioned stimuli of 4, 10, 16 or 40 kHz (60 dB SPL), and false positive responses were measured on the third day after salicylate injection. Each number of false positive responses was 0.6±0.4 (4 kHz), 2.8±0.8 (10 kHz), 4.2±0.9 (16 kHz), or 0.6±0.4 (40 kHz) and increased significantly when the conditioned stimulus was 16 kHz (* $P=0.004$) (Fig. 2A). Then, animals were also divided into three groups ($n=6$ in each group) according to conditioned stimuli of 20, 60 or 80 dB SPL (16

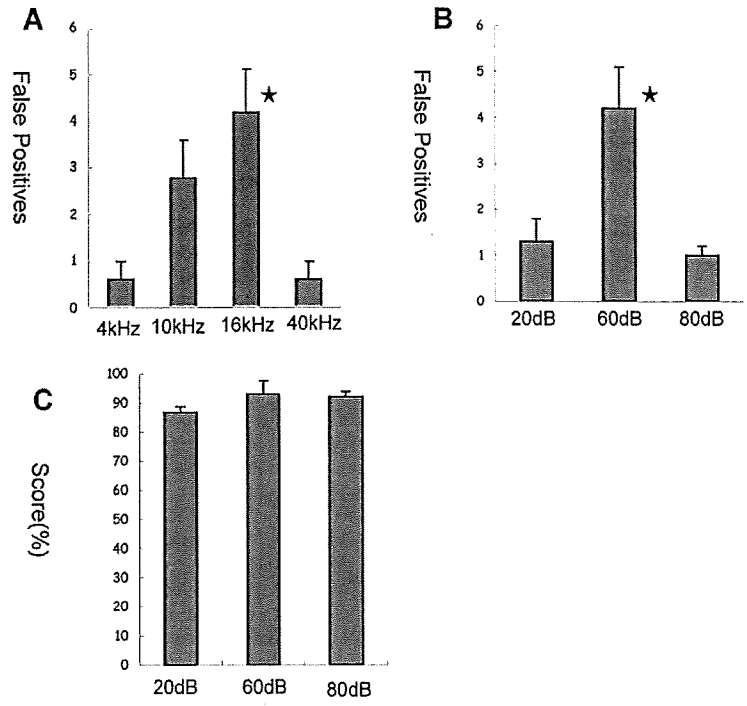

Fig. 2. The most appropriate kHz and dB sound pressure level (SPL) for the conditioning stimulus in the rat salicylate-induced tinnitus model. (A) Animals were divided into four groups (n=6 in each group) according to conditioning stimuli of 4, 10, 16 or 40 kHz (60 dB SPL). The number of false positives were measured on the third day after salicylate injection and increased significantly when the conditioning stimulus was 16 kHz (* P<0.005). (B) Animals were divided into three groups (n=6 in each group) according to conditioning stimuli of 20, 60 or 80 dB SPL (16 kHz). The number of false positives between these groups on the third day after salicylate injection increased significantly when the conditioning stimulus was at 60 dB SPL (* P<0.05). (C) The percentage of correct responses (score %) to sound of 20, 60 or 80 dB SPL (16 kHz) (active avoidance score). There were no significant differences between all three groups.

kHz) and false positive responses were measured as above. Each number of false positive responses was 1.3±0.5 (20 dB SPL), 4.2±0.9 (60 dB SPL), or 1.0±0.2 (80 dB SPL) and increased significantly when the conditioned stimulus was 60 dB SPL (* P=0.013) (Fig. 2B). The active avoidance score showed no significant change among all these groups, though (Fig. 2C). From these experiments, a 16 kHz and 60 dB SPL pure tone sound was adopted as the most appropriate conditioned stimulus for the present Wistar rat study.

Animals in the control group showed no significant change either in the active avoidance score (Fig. 3A) or in the false positive responses (Fig. 3B) from day 0 to day 4. The active avoidance scores of control and experimental

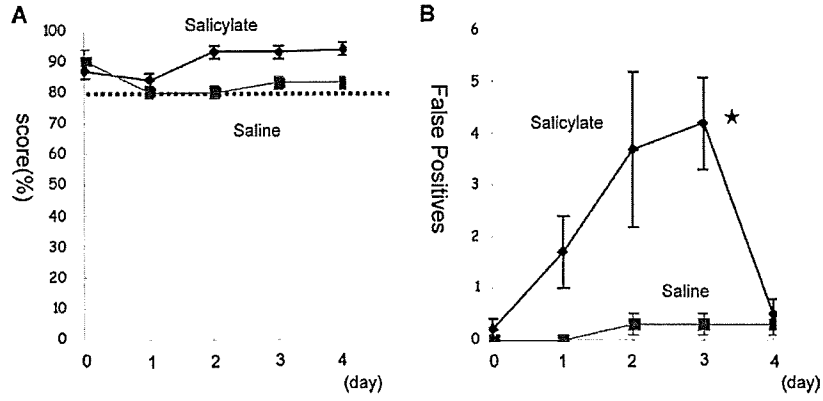

Fig. 3. The active avoidance score (A) and false positive responses (B) in salicylate-treated rats. (A) The percentage of correct responses to sound (active avoidance score %) measured before (day 0), during (day 1–3), and after injections of saline or salicylate (400 mg/kg i.p.) (day 4). The active avoidance score % remained stable (≥80%) in both groups during the experimental period. (B) The number of abnormal responses during silent periods (false positives). Injections of salicylate significantly increased the number of false positives on the third day (day 3) (* P<0.005). A complete recovery was seen when the treatment was stopped on the fourth day (day 4).

animals remained stable (≥80%) during the whole period of saline and salicylate administration. This suggests that salicylate application did not cause any obvious functional damage to cochlear endo-organs. False positive responses increased gradually after salicylate treatment with a maximum at day 3 (day 1: 0.2±0.2, day 2: 1.7±0.7, day 3: 4.2±0.9, day 4: 0.5±0.3, * P=0.002) and returned to the control value at day 4. This suggests that salicylate treatment caused a phantom sound sensation or "tinnitus" in rats, with a maximum at day 3 that endured for one day at most.

ABR assessment

We examined if the salicylate induced the inner ear dysfunction by means of ABR. We used the III wave in the measurement of ABR threshold, because this was most detectable at lower-intensity stimuli reference. No remarkable differences were observed between mean ABR threshold of control and salicylate-treated rats (data not shown). This suggests that salicylate treatment did not cause any obvious functional damage to cochlear endo-organs.

Morphological assessment

Neither hair cells nor SG cells showed any remarkable changes between control and salicylate-treated rats (data not shown). This suggests that salicylate treatment did not cause any obvious morphological damage to cochlear endo-organs.

Expression of TRPV1 in the auditory pathway and BRCx

TRPV1 mRNA levels in the SG were significantly upregulated 2 h (2.39±0.18 fold: * P=0.0005), returned to control levels 12 h (0.81±0.02 fold: P=0.105), significantly suppressed 24 h (0.35±0.03 fold: ** P=0.0002) and returned to control levels 72 h post-treatment (0.91±0.05 fold: P=0.130) (Fig. 4A). TRPV1 mRNA levels in the DCN were significantly suppressed 2 h (0.53±0.03 fold: * P=0.0001) and 12 h (0.64±0.03 fold: * P=0.0001) post-treatment, respectively and returned to control levels 24 h post-treatment (1.01±0.05 fold: P=0.810) (Fig. 4B). TRPV1 mRNA levels in the BRCx did not show any significant change after salicylate treatment (Fig. 4C).

TRPV1 protein levels in the inner ear

Fig. 5 illustrates western blot results for TRPV1 and the relative protein levels (TRPV1/actin in CONT=1) in the rat SG, DCN and BRCx. Similar to the results for mRNA levels, TRPV1 protein levels in the SG were significantly increased 2 h after salicylate treatment (2.94±0.72: * P=0.022) and returned to control levels 24 h after salicylate treatment (0.89±0.65: P=0.068) (Fig. 5A). In spite of a slight reduction 2 h after salicylate treatment (0.61±0.48: * P=0.044), TRPV1 protein levels in the DCN were significantly increased 24 h after salicylate treatment (1.56±0.60: ** P=0.038) (Fig. 5C). TRPV1 protein levels in the BRCx did not show any significant change after salicylate treatment (Fig. 5D).

TRPV1 immunoreactivity in the salicylate-treated group was clearly enhanced in almost all SG cells compared with that in the saline-control group (Fig. 5B). The dense immunoreactivity extended beyond the perinuclear region and into the somata of ganglion cells. All TRPV1 immunoreactivity was eliminated by pre-absorption with an excess of blocking peptide (data not shown).

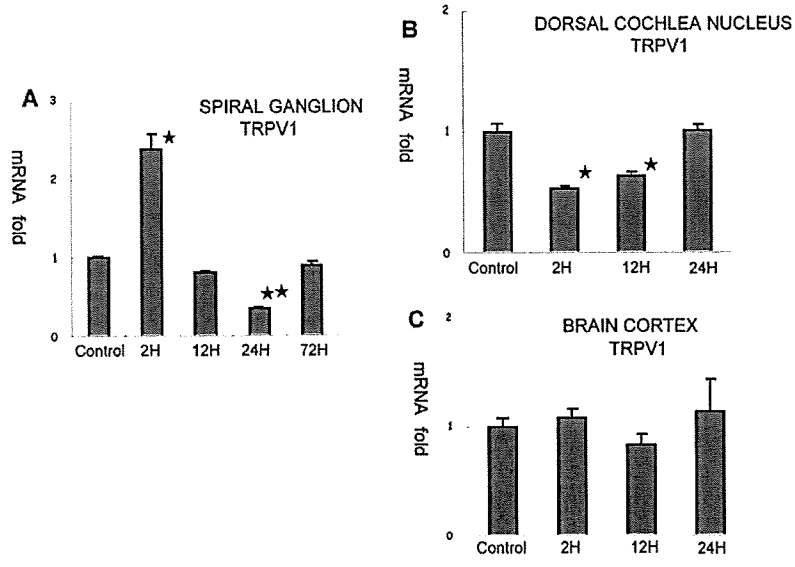

Fig. 4. Salicylate-induced changes in transient receptor potential cation channel superfamily V-1 (TRPV1) mRNA levels in the rat spiral ganglion (SG) (A), dorsal cochlear nucleus (DCN) (B) and brain cortex (BRCx) (C). (A) TRPV1 mRNA levels in SG were significantly upregulated 2 h (* P<0.001), returned to control levels 12 h, significantly suppressed 24 h (** P<0.0005) and returned to control levels 72 h post-treatment. (B) TRPV1 mRNA levels in the DCN were significantly suppressed at the 2 and 12 h post-treatment (* P<0.0005) and had returned to control levels 24 h post-treatment. (C) TRPV1 mRNA levels in the BRCx did not show any significant change after salicylate treatment.

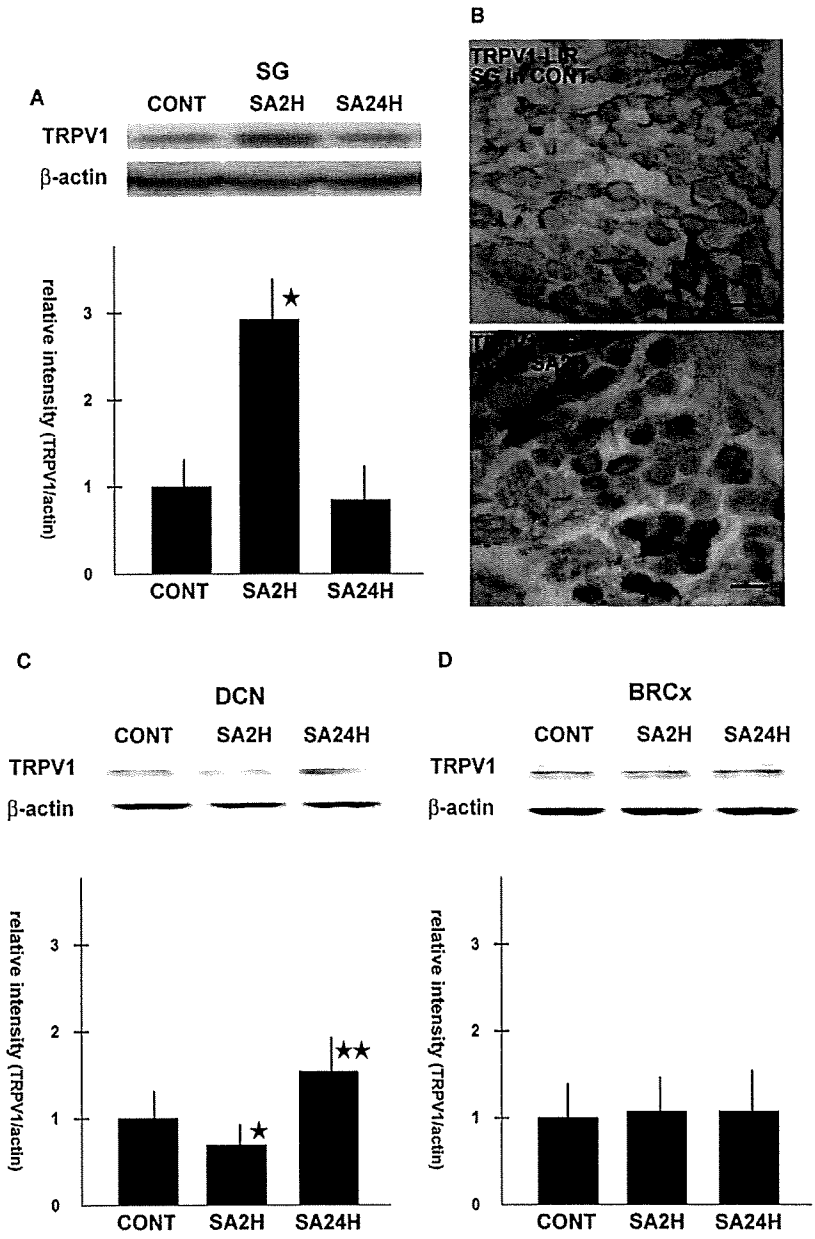

Fig. 5. Western blot analysis (A, C, D) and immunohistochemistry (B) of salicylate-induced changes in TRPV1 protein levels in the rat SG, DCN and BRCx. (A) TRPV1 protein levels in SG were significantly increased 2 h after salicylate treatment (SA2H) (* $P<0.05$) and had returned to control levels (CONT) 24 h after salicylate treatment (SA24H). (B) TRPV1-like immunoreactivity (LIR) in the salicylate-treated group (SA2H) was clearly enhanced in almost all SG cells compared with that in the saline-control group (CONT). (C) In spite of a slight reduction 2 h after salicylate treatment (SA2H) (* $P<0.05$), TRPV1 protein levels in the DCN were significantly increased 24 h after salicylate treatment (SA24H) (** $P<0.05$). (D) TRPV1 protein levels in the BRCx did not show any significant change after salicylate treatment.

Effect of TRPV1 antagonist

Behavioral assessment showed that false positive responses were increased 2 h post-treatment in group II (salicylate+DMSO) (3.7±1.2 responses) compared with control group I and that this increase was significantly suppressed in group III (salicylate+capsazepine) (0.8±0.5 responses, * $P=0.015$) (Fig. 6A). Examination of TRPV1 mRNA levels in the SG showed that mRNA was upregulated 2 h post-treatment in group II (salicylate+DMSO) (3.38±1.13 fold) compared with the control group I and that this upregulation was significantly suppressed in group III (salicylate+capsazepine) (0.85±0.07 fold, * $P=0.020$) (Fig. 6B). Capsazepine suppressed the salicylate-induced molecular changes in the SG in a dose dependent manner (Fig. 6C).

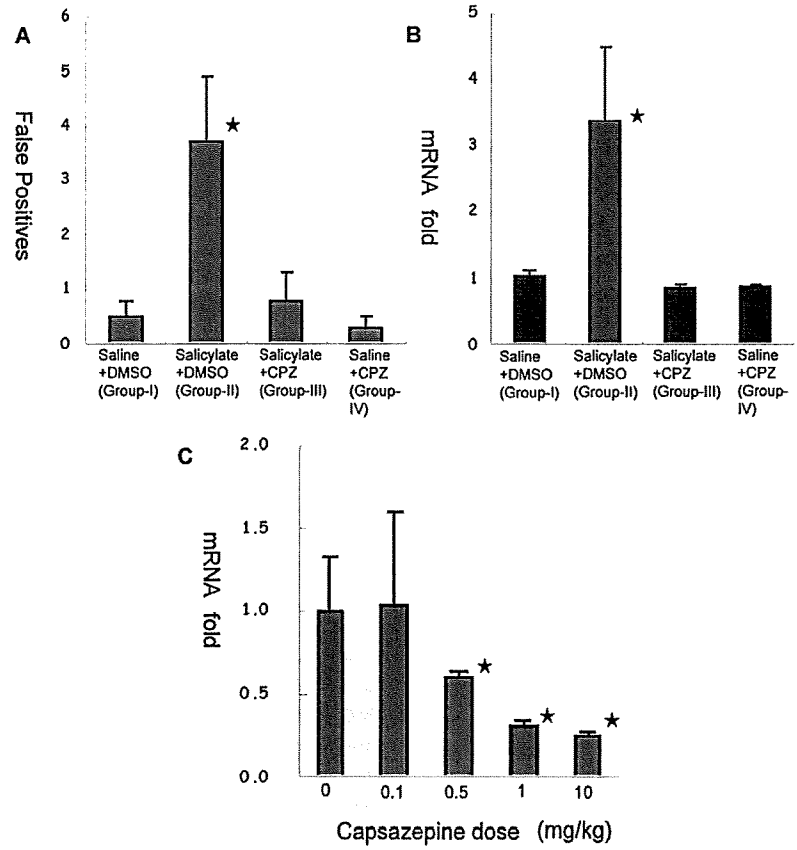

Fig. 6. Capsazepine (CPZ) blocked both the salicylate-induced increase of false positives and upregulation of TRPV1 mRNA in the rat SG. Dimethyl sulfoxide (DMSO) or CPZ (10 mg/kg i.p.) was administrated 0.5 h after the first injection of saline or salicylate. (A) False positives were increased 2 h post-treatment in group II (salicylate+DMSO) and this increase was significantly suppressed in group III (salicylate+CPZ) (* $P<0.05$). (B) TRPV1 mRNA was upregulated in the SG 2 h post-treatment in group II (salicylate+DMSO) and this upregulation was significantly suppressed in group III (salicylate+CPZ) (* $P<0.05$). (C) CPZ (0–10 mg/kg) suppressed the salicylate-induced upregulation of TRPV1 mRNA in the SG in a dose dependent manner (* $P<0.05$).

DISCUSSION

One of the reasons why it is still so hard for clinicians to cure intractable tinnitus is that appropriate animal models of tinnitus have not yet been established. To overcome this deficiency, we present here an animal behavioral model of tinnitus. Validating a behavioral procedure in animals to assess the presence of tinnitus is an unusual and difficult task to which many research groups have devoted many years. Among these groups, Jastreboff and Sasaki (1994) proposed an animal model based on an active avoidance paradigm; animals were conditioned by electrical footshock to drink water when hearing a sound. Recently, Guitton et al. (2003) demonstrated an animal model involving escape to a climbing pole to avoid electrical footshock when hearing a sound. In the present study, we further developed Guitton's model with modifications of a much easier active avoidance task of escaping to the next room instead. Adult or even aged animals were able to quickly step over the wall to move to the other side of the box. The conditioning box should also be set in a soundproof room, because it was important for animals to clearly hear both the conditioned sound and salicylate-induced phantom sound.

Previous studies in tinnitus kHz have revealed that salicylate induces an acute, relatively high frequency and transient type of tinnitus. It ranges from 10 to 16 kHz (Bauer et al., 1999; Guitton et al., 2003; Zheng et al., 2006; Yang et al., 2007). In the present study, false positive responses increased significantly when the conditioned stimulus was 16 kHz compared with 4, 10 and 40 kHz. Previous studies in tinnitus dB SPL have also shown that salicylate caused tinnitus of around 60 dB SPL (Bauer et al., 1999; Guitton et al., 2003; Rüttiger et al., 2003; Zheng et al., 2006; Yang et al., 2007). In the present study, false positive responses also increased significantly when the conditioned stimulus was 60 dB SPL compared with 20 dB SPL and 80 dB SPL. Judging from these pilot experiments, together with previous papers, 16 kHz and 60 dB SPL pure tone sound was the most similar to the sound of 400 mg/kg salicylate-induced tinnitus in the present Wistar rat study.